In vivo CRISPR screens identify novel virulence genes among proteins of unassigned subcellular localization in *Toxoplasma*

Yuta Tachibana[1,2], Miwa Sasai[1,2,3], and Masahiro Yamamoto[1,2,3]*

[1]Department of Immunoparasitology, Research Institute for Microbial Diseases,
[2]Laboratory of Immunoparasitology, WPI Immunology Frontier Research Center,
[3]Department of Immunoparasitology, Center for Infectious Disease Education and Research, Osaka University, Suita, Osaka 565-0871, Japan

Running title: *In vivo* CRISPR screens on hyperLOPIT-unassigned genes

Key words: *Toxoplasma, CRISPR screen, hyperLOPIT-unassigned virulence factors*

*Correspondence:
Masahiro Yamamoto
(E-mail: myamamoto@biken.osaka-u.ac.jp)

ABSTRACT

The research field to identify and characterize virulence genes in *Toxoplasma gondii* has been dramatically advanced by a series of *in vivo* CRISPR screens. Although subcellular localizations of thousands of proteins were predicted by the spatial proteomic method called hyperLOPIT, those of more than 1000 proteins remained unassigned and their essentiality in virulence was also unknown. In this study, we generated two small-scale gRNA libraries targeting approximately 600 hyperLOPIT-unassigned proteins and performed *in vivo* CRISPR screens. As a result, we identified several *in vivo* fitness-conferring genes that were previously unreported. We further characterized two candidates, TgGTPase and TgRimM, which are localized in the cytoplasm and the apicoplast, respectively. Both genes are essential for parasite virulence and widely conserved in the phylum Apicomplexa. Collectively, our current study provides a resource for estimating the *in vivo* essentiality of *Toxoplasma* proteins with previously unknown localizations.

IMPORTANCE

Toxoplasma gondii is a protozoan parasite that causes severe infection in immunocompromised patients or newborns. *Toxoplasma* possesses more than 8000 genes; however, the genes that determine parasite virulence were not fully identified. The apicomplexan parasites, including *Toxoplasma*, developed unique organelles that do not exist in other model organisms; thus, determining the subcellular location of parasite proteins is important for understanding their functions. Here, we used *in vivo* CRISPR genetic screens that enabled us to investigate hundreds of genes in *Toxoplasma* during mouse infection. We screened approximately 600 parasite proteins with previously unknown subcellular localizations. We identified many novel genes that confer parasite fitness in mice. Among the top hits, we characterized two essential virulence genes, TgGTPase and TgRimM, which are widely conserved in the phylum Apicomplexa. Our findings will contribute to understanding how apicomplexans adapt to the host environment and cause disease.

50 **INTRODUCTION**

51 An obligate intracellular parasite, *Toxoplasma gondii*, is an important human and
52 animal pathogen that causes life-threatening toxoplasmosis (1). *Toxoplasma* has been the
53 model apicomplexan parasite owing to its easiness of *in vitro* cultivation, genetic
54 tractability, *in vivo* disease model in mice, and various biological assays to investigate the
55 function of the genes (2). As unicellular eukaryotes that adapt to intracellular parasitism,
56 apicomplexans have developed unique secretory organelles (e.g., micronemes, rhoptries,
57 dense granules), which are absent in other well-studied eukaryotic cell systems (3). These
58 secretory organelles are key features of the apicomplexans and discharge various types of
59 proteins that are essential for invasion, replication, and egress (3). Likewise, the
60 apicoplast is a unique non-photosynthetic plastid-like organelle and essential for
61 apicomplexans' metabolism (fatty acid, heme, iron-sulfur cluster, and isoprenoid
62 synthesis) (4). Therefore, uncovering the subcellular localizations of parasite proteins is
63 crucial to understand the protein functions and parasite pathogenesis mechanism.

64 Although the parasite protein localization is typically revealed by cell biological
65 methods such as classical immunofluorescence assay (IFA), immuno-electron
66 microscopy, and, recently, ultrastructure expansion microscopy (U-ExM) (5, 6), the
67 parasite spatial proteome has been largely unknown. Recent studies elegantly addressed
68 the issues in *Toxoplasma* (7) and *Cryptosporidium* (8) by a spatial proteomic method
69 called hyperLOPIT (9), yielding plenty of knowledge on parasite subcellular proteome.
70 In a previous study using hyperLOPIT on *Toxoplasma* (7), approximately 3800 proteins
71 were identified in the tachyzoite stage; however, about 1,200 of them are still classified
72 as unassigned subcellular localizations. Moreover, the functions of these genes mostly
73 remained to be elucidated.

74 In addition to classical forward and reverse genetics, *in vitro* or *in vivo* CRISPR
75 genetic screens have been used to assess the essentiality of the parasite genes in the lytic
76 cycles or virulence (10-15). We previously performed *in vivo* CRISPR screens using
77 small-scaled guide RNA (gRNA) libraries based on hyperLOPIT-assigned localizations
78 (e.g., rhoptries, dense granules, nucleus, endoplasmic reticulum (ER), Golgi apparatus,
79 cytosol, apicoplast, and mitochondrion) and identified novel secreted and non-secreted
80 virulence factors (14). However, the essentiality of hyperLOPIT-unassigned proteins in

81 virulence remains mostly unknown.

82 In this study, we generated two small-scaled gRNA libraries targeting genes
83 encoding hyperLOPIT-unassigned proteins and performed *in vivo* CRISPR screens in
84 mice. We identified several novel genes that contribute to the parasite's *in vivo* fitness.
85 Among the top hits, we further focused on two candidates, TgGTPase (TGGT1_277840)
86 and TgRimM (TGGT1_321310). TgGTPase is a guanosine triphosphatase (GTPase) that
87 localizes in the parasite cytosol, and TgRimM is a novel apicoplast-resident protein
88 possessing a ribosome maturation factor M (RimM) domain and a C2H2-type zinc finger
89 domain. Both genes are widely conserved among the apicomplexans, and gene deletions
90 led to the complete loss of virulence in mice, suggesting that TgGTPase and TgRimM are
91 essential for the parasite adaptation to the *in vivo* environment. Overall, our current study
92 provides a clue for the research community to estimate the *in vivo* essentiality of proteins
93 with previously unknown localizations.

94

95 **RESULTS**

96 ***In vivo* CRISPR screening targeting proteins of unassigned subcellular localization**

97 To identify genes necessary for *Toxoplasma* survival in mice, we utilized a
98 previously established *in vivo* CRISPR screen platform using type I strain and C57BL/6
99 mice (14). We newly generated two gRNA libraries (Unassigned_1 and Unassigned_2
100 libraries), each targeting 295 genes classified as unassigned localization in hyperLOPIT
101 (7) and control genes for *in vitro* and *in vivo* selection. Among approximately 1200
102 hyperLOPIT-unassigned proteins, we excluded genes with previously published *in vitro*
103 fitness scores in human foreskin fibroblasts (HFF) less than -1.5 to reduce the size of
104 the gRNA library (10). Transfected RHΔhxgprt parasites were selected with
105 pyrimethamine in Vero cells for four passages to generate a pooled mutant population
106 (*in vitro* sample). The parasite mutant pools were used to infect C57BL/6 mice with 10^7
107 parasites each by injection into the footpad. After seven days post infection, parasites
108 were recovered from the spleen and expanded in Vero cells for one passage (*in vivo*
109 sample). The gRNA sequences were amplified by PCR from the input library and the
110 genomic DNA extracted from the parasites of *in vitro* and *in vivo* samples. The gRNAs
111 were sequenced by next-generation sequencing to determine their relative abundance.

112 We calculated *in vitro* and *in vivo* fitness scores of each gene as the average $\log_2$ fold
113 change of guide abundances between conditions. We analyzed the screen results from
114 both sublibraries to assess the reproducibility **(Tables S1 and S2)**. The *in vitro* essential
115 and dispensable controls were successfully separated, with lower scores for the essential
116 genes and higher scores for the dispensable genes (**Figure S1A**). The correlations
117 between our *in vitro* fitness scores and the genome-wide *in vitro* fitness scores in HFFs
118 were high (r = 0.78 and 0.76, respectively) (**Figure S1B**) (10). High reproducibility of
119 *in vivo* fitness scores was observed between independent infections in mice (r =
120 0.75±0.05 and 0.68±0.07, respectively) (**Figure S1C**). These data demonstrated that our
121 *in vitro* and *in vivo* CRISPR screens using Unassigned_1 and Unassigned_2 libraries
122 were highly reproducible.
123 To identify genes that confer parasite *in vivo* fitness during infection in mice,
124 we compared *in vitro* and *in vivo* fitness scores (**Figure 1A, Tables S1 and S2**). To
125 rank the candidate genes, we calculated the distance of each gene from the regression
126 line (**Figure 1B**). As reported previously (14), the *in vivo* essential controls ROP18 and
127 GRA23 showed negative *in vivo* fitness scores and ranked highly (**Figure 1B**). This
128 analysis highlighted both previously identified and unidentified genes. For instance, the
129 top hits from Unassigned_1 library contain hypothetical protein (TGGT1_211850),
130 thioredoxin (Txn: TGGT1_224060), NUDIX hydrolase (Nudix: TGGT1_282190),
131 CAAX metallo endopeptidase (Caax: TGGT1_221170), vacuolar iron transporter (VIT:
132 TGGT1_266800), DNA damage inducible protein 1 (DDI1: TGGT1_304680),
133 TgGTPase (TGGT1_277840), GLT2 (TGGT1_239752), apical annuli methyltransferase
134 (AAMT: TGGT1_310070), and mRNA cleavage factor family protein (mRNACF:
135 TGGT1_221190). It has been reported that VIT mainly localizes to the plant-like
136 vacuolar compartment (PLVAC) and regulates parasite iron metabolism (16). DDI1 is
137 one of the components of the parasite ubiquitin-proteasome system and is localized in
138 the cytoplasm and nucleus (17). TgGTPase was identified as an interactor of the Nd
139 complex, which facilitates rhoptry exocytosis (18). GLT2 is a glucosyltransferase and
140 required for parasite disaccharide metabolism (19). AAMT was identified as an apical
141 annuli component (20). The top hits from Unassigned_2 library also contain several
142 hypothetical proteins (TGGT1_300220, TGGT1_312840, TGGT1_277870,

143 TGGT1_250790, TGGT1_221640, and TGGT1_273905), ribosome maturation factor
144 RimM domain-containing protein (TgRimM: TGGT1_321310), TBC6
145 (TGGT1_237280), DnaJ domain-containing protein (Dnaj: TGGT1_203380), CPSF A
146 subunit region protein (CPSF: TGGT1_ 267710), and rRNA-processing protein
147 EFG1(EFG1: TGGT1_240660). Although TGGT1_300220 was also shown to be one of
148 the top hits in another *in vivo* CRISPR screen (15), no further investigation was
149 performed. TBC6 is one of the TBC-domain containing proteins and is localized in the
150 ER or cytoplasmic vesicles (21). TGGT1_273905 localizes to the cytoplasm (22).
151 Although some candidates (VIT and DDI1) were previously reported to be required for
152 parasite virulence (16, 17), none of the other top hits are assessed regarding virulence so
153 far.
154
155 **Identification of novel genes that contribute to parasite virulence in mice**
156 We generated individual knockout strains to examine whether these top-hit
157 genes affect parasite virulence (**Figures S2A and S2B**). WT mice were locally infected
158 with these mutant strains into the footpad, and the survival rates were monitored. We
159 chose footpad infection rather than intraperitoneal infection because our previous study
160 revealed that the former is more suitable for assessing virulence in using RH strain (14)
161 (**Figures 2A and 2B**). Among the candidates from Unassigned_1 library, all mice
162 survived in the infection of ΔTGGT1_211850, ΔDDI1, ΔTgGTPase, or ΔAAMT
163 parasites. Other tested mutants also showed reduced virulence (ΔGLT2, ΔCaax,
164 ΔmRNACF, ΔTxn, ΔNudix, and ΔVIT). Among the candidates from Unassigned_2
165 library, all mice survived in the infection of ΔTGGT1_300220, ΔTgRimM, ΔEFG1,
166 ΔCPSF, or ΔTGGT1_277870 parasites. ΔTGGT1_250790, ΔDnaj, ΔTGGT1_312840,
167 or ΔTGGT1_273905 parasites showed reduced virulence. WT mice infected with
168 ΔTBC6, and ΔTGGT1_221640 succumbed in a time course similar to those infected
169 with WT parasites. Collectively, these data demonstrated that our *in vivo* CRISPR
170 screens targeting hyperLOPIT-unassigned proteins highlighted known and novel *in vivo*
171 fitness-conferring genes that affect virulence.
172
173 **TgGTPase is a widely conserved GTPase that contributes to virulence**

174 Among the top-ranking candidates from Unassigned_1 library, we chose to
175 characterize TgGTPase further (**Figure 3A and Tables S1**). TgGTPase is a GTPase that
176 is broadly conserved across the phylum Apicomplexa (**Figures 3B and 3C**). To study
177 the function of TgGTPase, we complemented the ΔTgGTPase strain with C-terminal
178 HA-tagged TgGTPase expressed from the tubulin promoter that we will refer to as
179 "ΔTgGTPase::TgGTPase-HA" (**Figure 3D**). Western blot showed the band of
180 TgGTPase-HA at around 40 kDa (**Figure 3E**). The HA-tagged TgGTPase showed a
181 cytoplasmic localization by IFA (**Figure 3F**). To validate the essentiality of TgGTPase
182 on pathogenesis, we infected C57BL/6 mice intraperitoneally with 10^3 tachyzoites of
183 the WT, ΔTgGTPase, and ΔTgGTPase::TgGTPase-HA parasites and assessed mouse
184 survival (**Figure 3G**). All the mice intraperitoneally infected with ΔTgGTPase parasites
185 survived. By contrast, ΔTgGTPase::TgGTPase-HA parasites fully restored virulence as
186 well as WT parasites. Taken together, these results suggest that TgGTPase is a
187 cytoplasmic protein essential for virulence.
188
189 **TgRimM is a novel apicoplast-resident protein possessing C2H2 zinc finger that**
190 **contributes to virulence in mice**
191 Among the top-ranking candidates from Unassigned_2 library, we chose to
192 characterize TgRimM further (**Figure 4A and Tables S2**). TgRimM possesses a signal
193 peptide, a ribosome maturation factor RimM domain, and a single C2H2-type zinc finger
194 domain (**Figure 4B**) (23, 24). We searched for TgRimM homologs and found that they
195 are broadly conserved across the phylum Apicomplexa except for *Cryptosporidium* spp.
196 (**Figure 4C**). To characterize TgRimM, we complemented the ΔTgRimM strain with C-
197 terminal HA-tagged TgRimM expressed from the tubulin promoter that we will refer to
198 as "ΔTgRimM::TgRimM-HA" (**Figure 4D**). The HA-tagged TgRimM showed an
199 apicoplast localization co-stained with streptavidin (an apicoplast marker) by IFA (**Figure**
200 **4E**). Western blot against TgRimM-HA showed the main band at around 75 kDa,
201 probably a processed form of TgRimM (**Figure 4F**). To check the effect of TgRimM on
202 virulence, we infected C57BL/6 mice intraperitoneally with 10^3 tachyzoites of the WT,
203 ΔTgRimM, and ΔTgRimM::TgRimM-HA parasites and assessed the mouse survival. All
204 the mice intraperitoneally infected with ΔTgRimM parasites survived. In contrast,

205 ΔTgRimM::TgRimM-HA parasites restored virulence (**Figure 4G**). Next, we assessed
206 the importance of the C2H2-type zinc finger domain in TgRimM. We generated a
207 complemented strain lacking the C2H2 zinc finger (ΔTgRimM::TgRimM$^{\Delta ZF}$-HA)
208 (**Figure 4C**). Deleting the zinc finger domain did not alter the apicoplast localization of
209 TgRimM$^{\Delta ZF}$-HA (**Figure S3**). However, ΔTgRimM::TgRimM$^{\Delta ZF}$-HA could not restore
210 virulence (**Figure 4G**). Thus, these results suggest that TgRimM is essential for virulence
211 in mice and that the C2H2 zinc finger is indispensable for TgRimM function in the
212 apicoplast.
213
214 **DISCUSSION**
215 Despite much effort from the research community, many apicomplexan proteins
216 still need to be annotated owing to their uniqueness and absence in other model organisms.
217 The CRISPR screens enabled the researchers to investigate hundreds to thousands of
218 genes in *Toxoplasma* at once *in vitro* culture or *in vivo* infection to identify essential genes
219 for parasite growth, metabolism, drug resistance, differentiation, host-pathogen
220 interaction, and virulence (10-15, 25-33). Most *in vivo* CRISPR screens in *Toxoplasma*
221 have been focused on identifying secreted virulence effectors such as rhoptry bulb
222 proteins (ROPs) and dense granule proteins (GRAs) (11-13). However, recent studies are
223 in progress to search for non-secreted virulence factors by *in vivo* CRISPR screens (14,
224 15). In this study, we focused on the hyperLOPIT-unassigned proteins and performed *in*
225 *vivo* CRISPR screens to identify novel virulence factors in *Toxoplasma*. As a result, we
226 identified many candidate genes that were required for the parasite *in vivo* fitness in mice
227 and further characterized TgGTPase and TgRimM among them.
228 TgGTPase was originally reported as an interactor of the Nd complex, which
229 plays an important role in rhoptry secretion (18). However, considering that our study
230 revealed its distribution in the cytosol, TgGTPase might have broader functions than
231 rhoptry secretion. TgGTPase homologs are widely conserved across the phylum
232 Apicomplexa, suggesting that this GTPase is functionally important across the species in
233 the phylum. In the transposon mutagenesis screen in *Plasmodium falciparum* (34),
234 PfGTPase (PF3D7_1348100) possesses lower mutagenesis scores (Mutagenesis Index
235 Score = 0.316 and Mutagenesis Fitness Score = -2.437), suggesting that PfGTPase is

236 essential for optimal growth of asexual blood-stages *in vitro*. Future studies on TgGTPase
237 homologs in *Plasmodium* or *Cryptosporidium* will reveal their conserved function in the
238 phylum.

239 We identified TgRimM as an apicoplast-resident protein. A homolog in *P.*
240 *falciparum* (PfRimM: PF3D7_1032000) is also predicted to be localized in the apicoplast
241 by signal peptide prediction (35). In the transposon mutagenesis screen in *P. falciparum*
242 (34), PfRimM also possesses very low mutagenesis scores (Mutagenesis Index Score =
243 0.158 and Mutagenesis Fitness Score = -2.8), indicating that PfRimM is essential for
244 growth of asexual blood-stages *in vitro*. Assuming that RimM homologs in the phylum
245 Apicomplexa (ApiRimM) are located in the apicoplast, the lack of RimM homologs in
246 *Cryptosporidium* is reasonable because *Cryptosporidium* spp. are known to have lost the
247 apicoplast (36-38). RimM domain-containing protein was reported to regulate 16S rRNA
248 processing in bacteria (39). It is reported that a RimM domain-containing protein in
249 *Arabidopsis thaliana* (AtRimM) is located in the chloroplasts and contributes to rRNA
250 maturation and proteostasis (40). Considering that the apicoplast evolved from secondary
251 endosymbiosis (41) and that the zinc finger domain in TgRimM is essential for its
252 function in our study, ApiRimM might facilitate rRNA maturation and proteostasis in the
253 apicoplast. Previous studies on *Toxoplasma* apicoplast have shown that apicoplast
254 function is essential for the parasite *in vitro* survival and growth (42-44). Moreover,
255 apicoplast-assigned proteins in hyperLOPIT showed a small number of *in vitro*
256 dispensable proteins (7), also supporting its bare essentiality. In sharp contrast, other than
257 TgRimM, we previously identified two additional apicoplast-resident proteins (EF-P:
258 TGGT1_258380 and hypothetical protein: TGGT1_204350) that are dispensable for *in*
259 *vitro* fitness but essential for *in vivo* fitness in CRISPR screens (14). The presence of this
260 type of apicoplast proteins that are dispensable *in vitro* but indispensable *in vivo* might
261 imply unknown characteristics of the apicoplast. Considering that the apicoplast is a
262 potent drug target against toxoplasmosis and malaria (45), the presence of such apicoplast
263 proteins that are dispensable *in vitro* but indispensable *in vivo* might expand the range of
264 anti-toxoplasmosis and -malarial drug targets in the future. In combination with the
265 database of hyperLOPIT, *in vivo* CRISPR screens succeeded in identifying such "new
266 class" apicoplast proteins essential for virulence.

267 Limitations of our current study are that, although approximately 1,200 proteins
268 are classified as unassigned subcellular localizations in hyperLOPIT, our sublibraries
269 cover only half of them. Therefore, the remaining proteins still need to be addressed in
270 the future. Also, although we identified previously unreported virulence genes in this
271 study, their precise functions and localizations, other than TgGTPase and TgRimM,
272 mostly remained unaddressed. Future works will aim to characterize these remaining
273 proteins further.
274 In conclusion, our *in vivo* CRISPR screen platform provides a resource for the
275 community to identify virulence genes encoding proteins with previously unknown
276 localizations and functions.
277
278 **MATERIALS AND METHODS**
279 ***Toxoplasma* strains**
280 RHΔhxgprt (14), RHΔhxgprtΔku80 (46) and its derivatives of *Toxoplasma* were
281 maintained in Vero cells and passaged every 3 days using RPMI (Nacalai Tesque)
282 supplemented with 2 % heat-inactivated fetal bovine serum (FBS; JRH Bioscience), 100
283 U/ml penicillin and 0.1 mg/ml streptomycin (Nacalai Tesque) in incubators at 37°C and
284 5% CO_2.
285
286 **Host cell culture**
287 Vero cells were maintained in RPMI (Nacalai Tesque) supplemented with 10 %
288 heat-inactivated FBS, 100 U/ml penicillin and 0.1 mg/ml streptomycin (Nacalai Tesque)
289 in incubators at 37°C and 5% CO_2. Human foreskin fibroblasts (HFFs) were maintained
290 in DMEM (Nacalai Tesque) supplemented with 10% heat-inactivated FBS, 100 U/ml
291 penicillin and 0.1 mg/ml streptomycin (Nacalai Tesque) in incubators at 37°C and 5%
292 CO_2.
293
294 **Mice**
295 C57BL/6NCrSlc (C57BL/6N) mice were purchased from SLC. All experiments
296 were conducted in 8-10-week-old female mice. All animal experiments were conducted

297 with the approval of the Animal Research Committee of Research Institute for Microbial
298 Diseases in Osaka University.
299
300 ***In vitro* and *in vivo* pooled CRISPR screens**
301 The gRNA sequences of Unassigned_1 and Unassigned_2 sublibrary were
302 selected from the genome-wide gRNA library (10). The selected gRNA sequences were
303 cloned into the modified pU6-Universal vector by cloning a T2A, DHFR, T2A, and RFP
304 in frame with Cas9, where the expression of gRNA and Cas9-T2A-DHFR-T2A-RFP
305 cassettes was independently transcribed. The insertion of the selected gRNA sequences
306 into the vector was performed by VectorBuilder. The gRNA library (200 μg) was
307 linearized with NotI and transfected into approximately 1-2×10^8 RHΔhxgprt parasites
308 divided between four separate cuvettes. Then, transfected parasites were grown in 4×150-
309 mm dishes with confluent Vero cell monolayers. Pyrimethamine (Sigma) was added 24
310 h post transfection. All the parasites were passaged every 3 days until Passage 3 without
311 filtration. After 2 days (Passage 4), the parasites were syringe lysed, filtered, and counted
312 for genomic DNA preparation or for mouse infection. For genomic DNA preparation, at
313 least 1×10^8 parasites were pelleted and stored at -80 °C. For mouse infection, the parasites
314 were resuspended in PBS at a concentration of 2.5×10^8 parasites/ml. Then, 1×10^7
315 parasites in 40 μl PBS were injected into the footpad of each anesthetized mouse. Parasite
316 viability was determined by plaque assay. At 7 days post infection, the spleens were
317 collected and crushed by a plunger and passed through a cell strainer to make single cell
318 suspensions. Then, the suspensions were pelleted and added to 2×150-mm dishes per
319 spleen with confluent Vero cell monolayers. After 2-4 days, when the parasites
320 completely lysed out, they were filtered and counted. At least 1×10^8 parasites were
321 pelleted and stored at -80 °C. Parasite genomic DNA was extracted using the DNeasy
322 Blood and Tissue kit (Qiagen) according to the manufacturer's instructions. Integrated
323 gRNA sequences were PCR-amplified and barcoded with KOD FX Neo (TOYOBO)
324 using Primer 1 and Primer 2 (**Table S3**). Genomic DNA (1μg) was used for the template.
325 The resulting libraries were sequenced on a DNBSEQ-G400RS (MGI) using Primer 3
326 and Primer 4 (**Table S3)**.
327

328 **Bioinformatic analysis of the CRISPR screen**

329 Following demultiplexing, gRNA sequencing reads were aligned to the gRNA
330 library. The abundance of each gRNA was calculated and normalized to the total number
331 of aligned reads (47). For *in vitro* analysis, the $\log_2$ fold-change between the P4 sample
332 and the library was calculated for each gRNA. The fitness score for each gene was
333 calculated as the mean $\log_2$ fold change for the top five scoring guides. For *in vivo* analysis,
334 the $\log_2$ fold-change between each *in vivo* sample and the P4 sample was calculated for
335 each gRNA as described above. The median fitness score across mouse replicates was
336 used as the *in vivo* fitness score (14). For a given gene, gRNAs were compared using
337 Wilcoxon rank sum test between P4 vs WT mice. The p values for each test were adjusted
338 using the Benjamini-Hochberg method. The distance of each gene from the regression
339 line was calculated as below.

340 $$\boldsymbol{distance}\big(\boldsymbol{ax+by+c=0},(\boldsymbol{x_0},\boldsymbol{y_0})\big)=\frac{\boldsymbol{ax_0+b\,y_0+c}}{\sqrt{\boldsymbol{a^2+b^2}}}$$

341 All analyses were conducted by R (v4.1.1) with package stats (v3.6.2) and visualized by
342 ggplot2 (v3.4.0).

343

344 **Plasmid construction for knockout *Toxoplasma***

345 For construction of the CRISPR/Cas9 plasmids for targeting a gene of interest
346 (GOI), two oligonucleotide primers (GOI_gRNA1_F and GOI_gRNA1_R,
347 GOI_gRNA2_F and GOI_gRNA2_R) containing gRNA sequence were annealed and
348 cloned into BsaI site of the pU6-Universal vector (Addgene #52694). To generate a
349 construct for deleting the entire coding region of GOI, flanking regions of 60 bp of 5' and
350 3' outside the gRNAs were used to surround the genes. Forward and reverse primers with
351 homology to the floxed HXGPRT cassette and to the 5' and 3' coding sequence of the
352 GOI was used (GOI_homology_F and GOI_ homology _R). The primer sequences used
353 for the genetic disruption are shown in **Table S3**.

354

355 **Generation of gene knockout *Toxoplasma***

356 RHΔhxgprtΔku80 were filtered and resuspended in Cytomix (10mM KPO_4,
357 120mM KCl, 0.15 mM $CaCl_2$, 5mM $MgCl_2$, 25 mM HEPES, 2 mM EDTA). Parasites
358 were mixed with 50 µg of each gRNA1 and gRNA2 CRISPR plasmids with the PCR-

359 amplified targeting fragment for each GOI, and supplemented with 2 mM ATP, 5mM
360 GSH. Parasites were electroporated by GENE PULSER II (Bio-Rad Laboratories).
361 Transfected parasites were selected by 25 μg/ml mycophenolic acid (MPA) (Sigma) and
362 50 μg/ml Xanthine (Wako) to obtain stably resistant clones. Then, parasites were
363 subjected to limiting dilution in 96-well plates to isolate single clones. To confirm the
364 disruption of the gene, we analyzed the mRNA expression by quantitative RT-PCR.
365

366 **Complementation of TgGTPase and TgRimM**

367 To complement the ΔTgGTPase and ΔTgRimM parasites, TgGTPase, TgRimM,
368 and TgRimM$^{\Delta ZF}$ cDNA was generated by PCR amplification from cDNA of the RH strain.
369 The PCR products were inserted into the pUPRT plasmid vector, which possesses cDNA
370 of interest with SPOT and HA epitope tag driven by the tubulin promoter. Indicated
371 parasites were transfected with the pUPRT complementation vector and gRNA targeting
372 the UPRT locus, then selected by FUDR (Wako) (48). Isolated clones were examined for
373 protein expression by western blotting and IFA.
374

375 **TgGTPase and TgRimM phylogenetic analysis**

376 ToxoDB (23), VEuPathDB (49) and BLAST were searched for TgGTPase or
377 TgRimM homologs across the phylum Apicomplexa. Clustal Omega was used to align
378 obtained homologs (50). Phylogenetic trees were visualized by ggtree (v3.2.1) (51).
379

380 **Immunofluorescence assay**

381 HFFs were grown on coverslips, infected with parasites for 24-30 h, and fixed
382 in PBS containing 3.7% paraformaldehyde (PFA) for 10 min at room temperature. Cells
383 were permeabilized with PBS containing 0.1% Triton-X for 10 min and then blocked with
384 in PBS containing 3% BSA for 1 h at room temperature. Then, the coverslips were
385 incubated with the primary antibodies for 1 h, followed by incubation with appropriate
386 secondary antibodies, streptavidin and DAPI for 30 min. The coverslips were mounted
387 using PermaFluor (Thermo Scientific). Images were acquired by confocal laser
388 microscopy (Olympus FV3000 IX83). Primary antibodies used were mouse anti-HA.11

389 (BioLegend, 901514), rabbit anti-GAP45 (52), and Alexa Fluor 594 streptavidin
390 (Invitrogen, S11227).
391
392 **Assessment of *in vivo* virulence in mice**
393 Mice were infected with 10^3 tachyzoites in 200 µl (intra-peritoneum) or 40 µl
394 (intra-footpad) of PBS. Parasite viability was determined by plaque assay. The mouse
395 health condition and survival were monitored daily until 30 days (intra-peritoneum) or 40
396 days (intra-footpad) post infection, respectively.
397
398 **Quantitative RT-PCR**
399 Total RNA was extracted by RNeasy kit (QIAGEN), and cDNA was synthesized
400 by Verso reverse transcription (Thermo Fisher Scientic) according to the manufacturer's
401 instructions. Quantitative RT-PCR was performed with a CFX Connect real-time PCR
402 system (Bio-Rad Laboratories) and a Go-Taq real-time PCR system (Promega). The data
403 were analyzed by the ΔΔCT method and normalized to ACT1 in each sample. The primer
404 sequences are listed in **Table S3**.
405
406 **Western blotting**
407 Cells were lysed in lysis buffer (1% NP-40, 150 mM NaCl, 20 mM Tris-HCl, pH
408 7.5) containing a protease inhibitor cocktail (Nacalai Tesque). The cell lysates were
409 separated by SDS-PAGE and transferred to polyvinylidene difluoride membranes
410 (Immobilon-P; Millipore). Membranes were blocked in 5% skim milk in 0.05% Tween-
411 20 in PBS for 1 h at room temperature, followed by incubation with primary antibodies
412 for 1 h at room temperature. Blots were then incubated with appropriate secondary
413 antibodies for 1 h at room temperature. Primary antibodies used were mouse anti-HA
414 (MBL, M180-7) and rabbit anti-ROP18 (this study).
415
416 **Generation of custom anti-ROP18 antibody**
417 Custom anti-ROP18 antibody (rabbit polyclonal) was generated against a synthetic C-
418 terminal peptide of ROP18 (AQNFEQQEHLHTE). The epitope identification, peptide

synthesis, rabbit immunization and serum collection were conducted by Cosmo Bio. The specificity of anti-ROP18 antibody was validated for western blotting.

Quantification and statistical analysis

Information about the number of biological replicates and the type of statistical tests used can be found in the figure legends. All statistical analyses except for the survival rates were performed using R (4.1.1, https://www.r-project.org/). For correlation analysis, Pearson's correlation was used. Data with p values < 0.05 were considered statistically significant. The statistical analysis of survival rates was performed by the log-rank test using the GraphPad Prism9 software.

Data availability

The CRISPR screen data of two sublibraries have been deposited to the NCBI GEO. The GEO accession numbers are **GSE253884** and **GSE253885**. Any additional information required to reanalyze the data reported in this paper is available from the corresponding author upon request.

ACKNOWLEGDEMENT

We thank M. Enomoto and N. Yamagishi (Osaka University) for secretarial and technical assistance. We acknowledge the NGS core facility at the Research Institute for Microbial Diseases of Osaka University for the sequencing. We thank Dr. D. Soldati-Favre for anti-GAP45 antibody. This study was supported by Fusion Oriented Research for Disruptive Science and Technology (JPMJFR206D), and Moonshot research & development (JPMJMS2025) from Japan Science and Technology Agency, the Research Program on Emerging and Re-emerging Infectious Diseases (JP23fk0108682) from the Agency for Medical Research and Development (AMED), a Grant-in-Aid for Transformative Research Area (B) (Establishment of PLAMP as a new concept to determine self and nonself for obligatory intracellular pathogens; 20B304), for Scientific Research (A) (19H00970), for JSPS Research Fellow (23KJ1469) from the Ministry of Education, Culture, Sports, Science and Technology, program from Joint Usage and Joint Research Programs of the Institute of Advanced Medical Sciences, Tokushima University,

Takeda Science Foundation, Mochida Memorial Foundation, Astellas Foundation for Research on Metabolic Disorders, Naito Foundation, the Chemo-Sero-Therapeutic Research Institute, Research Foundation for Microbial Diseases of Osaka University, BIKEN Taniguchi Scholarship, and Joint Research Program of Research Center for Global and Local Infectious Diseases of Oita University (2021B06).

AUTHOR CONTRIBUTIONS

Conceptualization, Y.T. and M.Y.; Methodology, Y.T. and M.Y.; Software and Formal Analysis, Y.T.; Investigation, Y.T. and M.Y.; Writing – Original Draft, Y.T. and M.Y.; Writing – Review & Editing, Y.T., M.S. and M.Y.; Funding Acquisition, M.Y.; Supervision, M.Y.

FIGURE LEGENDS

Figure 1. *In vivo* CRISPR screening targeting proteins with hyperLOPIT-unassigned localization.

(A) Scatterplots showing in vitro and in vivo fitness scores from Unnassigned_1 (left) and Unassigned_2 (right) libraries, respectively. ROP18 and GRA23 are labeled in orange as control genes.

(B) Ranking tables for top 15 *in vivo* fitness-conferring genes in each library ordered by the distance from the regression line.

Figure 2. Validation of candidate genes that affect parasite virulence.

(A) C57BL/6 mice were inoculated into the footpad with 10^3 tachyzoites of the indicated knockout strains from the unassigned_1 library. WT (n = 6), ΔTGGT1_211850 (n = 5), ΔDDI1 (n = 5), ΔTgGTPase (n = 5), ΔAAMT (n = 5), ΔGLT2 (n = 5), ΔCaax (n = 5), ΔmRNACF (n = 5), ΔTxn (n = 5), ΔNudix (n = 5), ΔVIT (n = 5).

(B) C57BL/6 mice were inoculated into the footpad with 10^3 tachyzoites of the indicated knockout strains from the unassigned_2 library. WT (n = 6), ΔTGGT1_300220 (n = 5), ΔTgRimM (n = 5), ΔEFG1 (n = 5), ΔCPSF (n = 5), ΔTGGT1_277870 (n = 5), ΔTGGT1_250790 (n = 5), ΔDnaj (n = 5), ΔTGGT1_312840 (n = 5), ΔTGGT1_273905 (n = 5), ΔTBC6 (n = 5), ΔTGGT1_221640 (n = 5). N.S., not significant (log-rank test).

481

482 **Figure 3. TgGTPase is a cytosolic GTPase that contributes to parasite virulence.**

483 (A) Rank-ordered plot of genes from Unassigned_1 library.

484 (B) Schematic of putative domains in TgGTPase.

485 (C) Phylogenetic tree of selected TgGTPase homologs across the apicomplexan phylum.

486 (D) Schematic of TgGTPase knockout and complementation of TgGTPase-HA.

487 (E) Western blot analysis of TgGTPase-HA.

488 (F) Immunofluorescence images of ΔTgGTPase::TgGTPase-HA showing cytosolic
489 localization of TgGTPase-HA (green). GAP45 (magenta) stains the inner membrane
490 complex of the parasites.

491 (G) Survival curves of C57BL/6 mice intraperitoneally infected with 10^3 tachyzoites of
492 WT (n = 5), ΔTgGTPase (n = 5), and ΔTgGTPase::TgGTPase-HA (n = 5).

493 Data are representative of three independent experiments (E and F).

494

495 **Figure 4. TgRimM is an apicoplast-resident protein that is essential for parasite**
496 **virulence.**

497 (A) Rank-ordered plot of genes from Unassigned_2 library.

498 (B) Schematic of putative domains in TgRimM. SP is predicted by SignalP 6.0.

499 (C) Phylogenetic tree of selected TgRimM homologs across the apicomplexan phylum.

500 (D) Schematic of TgRimM knockout and complementation of wild-type and mutant
501 TgRimM.

502 (E) Immunofluorescence images of ΔTgRimM::TgRimM-HA showing TgRimM-HA
503 (green) is co-stained with streptavidin (magenta), an apicoplast marker.

504 (F) Western blot analysis of TgRimM-HA.

505 (G) Survival curves of C57BL/6 mice intraperitoneally infected with 10^3 tachyzoites of
506 WT (n = 5), ΔTgRimM (n = 5), ΔTgRimM::TgRimM-HA (n = 5), or
507 ΔTgRimM::TgRimM$^{\Delta ZF}$-HA (n = 5).

508 Data are representative of three independent experiments (E and F).

509

510 **SUPPLEMENTAL MATERIAL**

511 **Supplementary Figure 1. Assessing the reproducibility of CRISPR screens.**

Related to Figure 1.

(A) Rank-ordered plots for *in vitro* fitness scores of 4th passage.

(B) Correlation between our *in vitro* fitness scores and the *in vitro* fitness scores in HFF.

(C) Overlay of *in vivo* fitness scores for each mouse. Pearson's correlation coefficients are shown as mean ± SD.

Supplementary Figure 2. Generating gene knockout parasites.

Related to Figure 2.

(A) Schematic of gene knockout strategy.

(B) Quantitative RT-PCR validations for indicated parasites.

Supplementary Figure 3. TgRimM$^{\Delta ZF}$-HA localized in the apicoplast.

Related to Figure 4.

Immunofluorescence images of ΔTgRimM::TgRimM$^{\Delta ZF}$-HA showing TgRimM$^{\Delta ZF}$-HA (green) is co-stained with streptavidin (magenta), an apicoplast marker. Data are representative of three independent experiments.

Table S1.

Summary of *in vivo* CRISPR screen using Unassigned_1 library, gRNA sequences, raw count data, and *in vivo* fitness scores for each mouse.

Table S2.

Summary of *in vivo* CRISPR screen using Unassigned_2 library, gRNA sequences, raw count data, and *in vivo* fitness scores for each mouse.

Table S3.

Lists of the primers used in this study.

REFERENCES

1. Montoya JG, Liesenfeld O. 2004. Toxoplasmosis. Lancet 363:1965-76.
2. Kim K, Weiss LM. 2004. Toxoplasma gondii: the model apicomplexan. Int J Parasitol 34:423-32.
3. Lebrun M, Carruthers VB, Cesbron-Delauw M-F. 2020. Toxoplasma secretory proteins and their roles in parasite cell cycle and infection, p 607-704, Toxoplasma gondii. Elsevier.

544 4. Kloehn J, Lacour CE, Soldati-Favre D. 2021. The metabolic pathways and transporters of
545 the plastid organelle in Apicomplexa. Curr Opin Microbiol 63:250-258.
546 5. Gambarotto D, Zwettler FU, Le Guennec M, Schmidt-Cernohorska M, Fortun D, Borgers
547 S, Heine J, Schloetel JG, Reuss M, Unser M, Boyden ES, Sauer M, Hamel V, Guichard P.
548 2019. Imaging cellular ultrastructures using expansion microscopy (U-ExM). Nat
549 Methods 16:71-74.
550 6. Tosetti N, Dos Santos Pacheco N, Bertiaux E, Maco B, Bournonville L, Hamel V, Guichard
551 P, Soldati-Favre D. 2020. Essential function of the alveolin network in the subpellicular
552 microtubules and conoid assembly in Toxoplasma gondii. Elife 9.
553 7. Barylyuk K, Koreny L, Ke H, Butterworth S, Crook OM, Lassadi I, Gupta V, Tromer E,
554 Mourier T, Stevens TJ, Breckels LM, Pain A, Lilley KS, Waller RF. 2020. A Comprehensive
555 Subcellular Atlas of the Toxoplasma Proteome via hyperLOPIT Provides Spatial Context
556 for Protein Functions. Cell Host Microbe 28:752-766 e9.
557 8. Guerin A, Strelau KM, Barylyuk K, Wallbank BA, Berry L, Crook OM, Lilley KS, Waller
558 RF, Striepen B. 2023. Cryptosporidium uses multiple distinct secretory organelles to
559 interact with and modify its host cell. Cell Host Microbe 31:650-664 e6.
560 9. Christoforou A, Mulvey CM, Breckels LM, Geladaki A, Hurrell T, Hayward PC, Naake T,
561 Gatto L, Viner R, Martinez Arias A, Lilley KS. 2016. A draft map of the mouse pluripotent
562 stem cell spatial proteome. Nat Commun 7:8992.
563 10. Sidik SM, Huet D, Ganesan SM, Huynh MH, Wang T, Nasamu AS, Thiru P, Saeij JPJ,
564 Carruthers VB, Niles JC, Lourido S. 2016. A Genome-wide CRISPR Screen in Toxoplasma
565 Identifies Essential Apicomplexan Genes. Cell 166:1423-1435 e12.
566 11. Young J, Dominicus C, Wagener J, Butterworth S, Ye X, Kelly G, Ordan M, Saunders B,
567 Instrell R, Howell M, Stewart A, Treeck M. 2019. A CRISPR platform for targeted in vivo
568 screens identifies Toxoplasma gondii virulence factors in mice. Nat Commun 10:3963.
569 12. Sangare LO, Olafsson EB, Wang Y, Yang N, Julien L, Camejo A, Pesavento P, Sidik SM,
570 Lourido S, Barragan A, Saeij JPJ. 2019. In Vivo CRISPR Screen Identifies TgWIP as a
571 Toxoplasma Modulator of Dendritic Cell Migration. Cell Host Microbe 26:478-492 e8.
572 13. Butterworth S, Torelli F, Lockyer EJ, Wagener J, Song OR, Broncel M, Russell MRG,
573 Moreira-Souza ACA, Young JC, Treeck M. 2022. Toxoplasma gondii virulence factor
574 ROP1 reduces parasite susceptibility to murine and human innate immune restriction.
575 PLoS Pathog 18:e1011021.
576 14. Tachibana Y, Hashizaki E, Sasai M, Yamamoto M. 2023. Host genetics highlights IFN-
577 gamma-dependent Toxoplasma genes encoding secreted and non-secreted virulence
578 factors in in vivo CRISPR screens. Cell Rep 42:112592.
579 15. Giuliano CJ, Wei KJ, Harling FM, Waldman BS, Farringer MA, Boydston EA, Lan TCT,

580 Thomas RW, Herneisen AL, Sanderlin AG, Coppens I, Dvorin JD, Lourido S. 2023.
581 Functional profiling of the Toxoplasma genome during acute mouse infection. bioRxiv
582 doi:10.1101/2023.03.05.531216.
583 16. Aghabi D, Sloan M, Gill G, Hartmann E, Antipova O, Dou Z, Guerra AJ, Carruthers VB,
584 Harding CR. 2023. The vacuolar iron transporter mediates iron detoxification in
585 Toxoplasma gondii. Nat Commun 14:3659.
586 17. Zhang H, Liu J, Ying Z, Li S, Wu Y, Liu Q. 2020. Toxoplasma gondii UBL-UBA shuttle
587 proteins contribute to the degradation of ubiquitinylated proteins and are important for
588 synchronous cell division and virulence. FASEB J 34:13711-13725.
589 18. Aquilini E, Cova MM, Mageswaran SK, Dos Santos Pacheco N, Sparvoli D, Penarete-
590 Vargas DM, Najm R, Graindorge A, Suarez C, Maynadier M, Berry-Sterkers L, Urbach S,
591 Fahy PR, Guerin AN, Striepen B, Dubremetz JF, Chang YW, Turkewitz AP, Lebrun M.
592 2021. An Alveolata secretory machinery adapted to parasite host cell invasion. Nat
593 Microbiol 6:425-434.
594 19. Gas-Pascual E, Ichikawa HT, Sheikh MO, Serji MI, Deng B, Mandalasi M, Bandini G,
595 Samuelson J, Wells L, West CM. 2019. CRISPR/Cas9 and glycomics tools for Toxoplasma
596 glycobiology. J Biol Chem 294:1104-1125.
597 20. Engelberg K, Chen CT, Bechtel T, Sanchez Guzman V, Drozda AA, Chavan S, Weerapana
598 E, Gubbels MJ. 2020. The apical annuli of Toxoplasma gondii are composed of coiled-coil
599 and signalling proteins embedded in the inner membrane complex sutures. Cell Microbiol
600 22:e13112.
601 21. Quan JJ, Nikolov LA, Sha J, Wohlschlegel JA, Bradley PJ. 2023. Toxoplasma gondii
602 encodes an array of TBC-domain containing proteins including an essential regulator that
603 targets Rab2 in the secretory pathway. bioRxiv doi:10.1101/2023.05.28.542599.
604 22. Roumegous C, Abou Hammoud A, Fuster D, Dupuy JW, Blancard C, Salin B, Robinson
605 DR, Renesto P, Tardieux I, Frenal K. 2022. Identification of new components of the basal
606 pole of Toxoplasma gondii provides novel insights into its molecular organization and
607 functions. Front Cell Infect Microbiol 12:1010038.
608 23. Harb OS, Roos DS. 2020. ToxoDB: Functional Genomics Resource for Toxoplasma and
609 Related Organisms. Methods Mol Biol 2071:27-47.
610 24. Teufel F, Almagro Armenteros JJ, Johansen AR, Gislason MH, Pihl SI, Tsirigos KD,
611 Winther O, Brunak S, von Heijne G, Nielsen H. 2022. SignalP 6.0 predicts all five types
612 of signal peptides using protein language models. Nat Biotechnol 40:1023-1025.
613 25. Butterworth S, Kordova K, Chandrasekaran S, Thomas KK, Torelli F, Lockyer EJ, Edwards
614 A, Goldstone R, Koshy AA, Treeck M. 2023. High-throughput identification of
615 Toxoplasma gondii effector proteins that target host cell transcription. Cell Host Microbe

616 31:1748-1762 e8.
617 26. Chen Y, Liu Q, Xue JX, Zhang MY, Geng XL, Wang Q, Jiang W. 2021. Genome-Wide
618 CRISPR/Cas9 Screen Identifies New Genes Critical for Defense Against Oxidant Stress
619 in Toxoplasma gondii. Front Microbiol 12:670705.
620 27. Harding CR, Sidik SM, Petrova B, Gnadig NF, Okombo J, Herneisen AL, Ward KE,
621 Markus BM, Boydston EA, Fidock DA, Lourido S. 2020. Genetic screens reveal a central
622 role for heme metabolism in artemisinin susceptibility. Nat Commun 11:4813.
623 28. Krishnamurthy S, Maru P, Wang Y, Bitew MA, Mukhopadhyay D, Yamaryo-Botte Y,
624 Paredes-Santos TC, Sangare LO, Swale C, Botte CY, Saeij JPJ. 2023. CRISPR Screens
625 Identify Toxoplasma Genes That Determine Parasite Fitness in Interferon Gamma-
626 Stimulated Human Cells. mBio 14:e0006023.
627 29. Krishnan A, Kloehn J, Lunghi M, Chiappino-Pepe A, Waldman BS, Nicolas D, Varesio E,
628 Hehl A, Lourido S, Hatzimanikatis V, Soldati-Favre D. 2020. Functional and
629 Computational Genomics Reveal Unprecedented Flexibility in Stage-Specific Toxoplasma
630 Metabolism. Cell Host Microbe 27:290-306 e11.
631 30. Lockyer EJ, Torelli F, Butterworth S, Song OR, Howell S, Weston A, East P, Treeck M.
632 2023. A heterotrimeric complex of Toxoplasma proteins promotes parasite survival in
633 interferon gamma-stimulated human cells. PLoS Biol 21:e3002202.
634 31. Paredes-Santos TC, Bitew MA, Swale C, Rodriguez F, Krishnamurthy S, Wang Y, Maru P,
635 Sangare LO, Saeij JPJ. 2023. Genome-wide CRISPR screen identifies genes synthetically
636 lethal with GRA17, a nutrient channel encoding gene in Toxoplasma. PLoS Pathog
637 19:e1011543.
638 32. Waldman BS, Schwarz D, Wadsworth MH, 2nd, Saeij JP, Shalek AK, Lourido S. 2020.
639 Identification of a Master Regulator of Differentiation in Toxoplasma. Cell 180:359-372
640 e16.
641 33. Wang Y, Sangare LO, Paredes-Santos TC, Hassan MA, Krishnamurthy S, Furuta AM,
642 Markus BM, Lourido S, Saeij JPJ. 2020. Genome-wide screens identify Toxoplasma gondii
643 determinants of parasite fitness in IFNgamma-activated murine macrophages. Nat
644 Commun 11:5258.
645 34. Zhang M, Wang C, Otto TD, Oberstaller J, Liao X, Adapa SR, Udenze K, Bronner IF,
646 Casandra D, Mayho M, Brown J, Li S, Swanson J, Rayner JC, Jiang RHY, Adams JH. 2018.
647 Uncovering the essential genes of the human malaria parasite Plasmodium falciparum by
648 saturation mutagenesis. Science 360.
649 35. Cilingir G, Broschat SL, Lau AO. 2012. ApicoAP: the first computational model for
650 identifying apicoplast-targeted proteins in multiple species of Apicomplexa. PLoS One
651 7:e36598.

652 36. Abrahamsen MS, Templeton TJ, Enomoto S, Abrahante JE, Zhu G, Lancto CA, Deng M,
653 Liu C, Widmer G, Tzipori S, Buck GA, Xu P, Bankier AT, Dear PH, Konfortov BA, Spriggs
654 HF, Iyer L, Anantharaman V, Aravind L, Kapur V. 2004. Complete genome sequence of
655 the apicomplexan, Cryptosporidium parvum. Science 304:441-5.
656 37. Xu P, Widmer G, Wang Y, Ozaki LS, Alves JM, Serrano MG, Puiu D, Manque P, Akiyoshi
657 D, Mackey AJ, Pearson WR, Dear PH, Bankier AT, Peterson DL, Abrahamsen MS, Kapur
658 V, Tzipori S, Buck GA. 2004. The genome of Cryptosporidium hominis. Nature 431:1107-
659 12.
660 38. Zhu G, Marchewka MJ, Keithly JS. 2000. Cryptosporidium parvum appears to lack a
661 plastid genome. Microbiology (Reading) 146 (Pt 2):315-321.
662 39. Bylund GO, Wipemo LC, Lundberg LA, Wikstrom PM. 1998. RimM and RbfA are
663 essential for efficient processing of 16S rRNA in Escherichia coli. J Bacteriol 180:73-82.
664 40. Liu K, Lee KP, Duan J, Kim EY, Singh RM, Di M, Meng Z, Kim C. 2023. Cooperative role
665 of AtRsmD and AtRimM proteins in modification and maturation of 16S rRNA in plastids.
666 Plant J 114:310-324.
667 41. van Dooren GG, Striepen B. 2013. The algal past and parasite present of the apicoplast.
668 Annu Rev Microbiol 67:271-89.
669 42. Leveque MF, Berry L, Cipriano MJ, Nguyen HM, Striepen B, Besteiro S. 2015.
670 Autophagy-Related Protein ATG8 Has a Noncanonical Function for Apicoplast
671 Inheritance in Toxoplasma gondii. mBio 6:e01446-15.
672 43. Niu Z, Ye S, Liu J, Lyu M, Xue L, Li M, Lyu C, Zhao J, Shen B. 2022. Two apicoplast
673 dwelling glycolytic enzymes provide key substrates for metabolic pathways in the
674 apicoplast and are critical for Toxoplasma growth. PLoS Pathog 18:e1011009.
675 44. Sanchez SG, Bassot E, Cerutti A, Mai Nguyen H, Aida A, Blanchard N, Besteiro S. 2023.
676 The apicoplast is important for the viability and persistence of Toxoplasma gondii
677 bradyzoites. Proc Natl Acad Sci U S A 120:e2309043120.
678 45. McFadden GI, Yeh E. 2017. The apicoplast: now you see it, now you don't. Int J Parasitol
679 47:137-144.
680 46. Huynh MH, Carruthers VB. 2009. Tagging of endogenous genes in a Toxoplasma gondii
681 strain lacking Ku80. Eukaryot Cell 8:530-9.
682 47. Sidik SM, Huet D, Lourido S. 2018. CRISPR-Cas9-based genome-wide screening of
683 Toxoplasma gondii. Nat Protoc 13:307-323.
684 48. Shen B, Brown KM, Lee TD, Sibley LD. 2014. Efficient gene disruption in diverse strains
685 of Toxoplasma gondii using CRISPR/CAS9. mBio 5:e01114-14.
686 49. Alvarez-Jarreta J, Amos B, Aurrecoechea C, Bah S, Barba M, Barreto A, Basenko EY,
687 Belnap R, Blevins A, Bohme U, Brestelli J, Brown S, Callan D, Campbell LI, Christophides

688 GK, Crouch K, Davison HR, DeBarry JD, Demko R, Doherty R, Duan Y, Dundore W,
689 Dyer S, Falke D, Fischer S, Gajria B, Galdi D, Giraldo-Calderon GI, Harb OS, Harper E,
690 Helb D, Howington C, Hu S, Humphrey J, Iodice J, Jones A, Judkins J, Kelly SA, Kissinger
691 JC, Kittur N, Kwon DK, Lamoureux K, Li W, Lodha D, MacCallum RM, Maslen G,
692 McDowell MA, Myers J, Nural MV, Roos DS, et al. 2024. VEuPathDB: the eukaryotic
693 pathogen, vector and host bioinformatics resource center in 2023. Nucleic Acids Res
694 52:D808-D816.
695 50. Sievers F, Wilm A, Dineen D, Gibson TJ, Karplus K, Li W, Lopez R, McWilliam H,
696 Remmert M, Soding J, Thompson JD, Higgins DG. 2011. Fast, scalable generation of
697 high-quality protein multiple sequence alignments using Clustal Omega. Mol Syst Biol
698 7:539.
699 51. Yu G. 2020. Using ggtree to Visualize Data on Tree-Like Structures. Curr Protoc
700 Bioinformatics 69:e96.
701 52. Plattner F, Yarovinsky F, Romero S, Didry D, Carlier MF, Sher A, Soldati-Favre D. 2008.
702 Toxoplasma profilin is essential for host cell invasion and TLR11-dependent induction of
703 an interleukin-12 response. Cell Host Microbe 3:77-87.
704

Figure 1 _Tachibana et al.

A

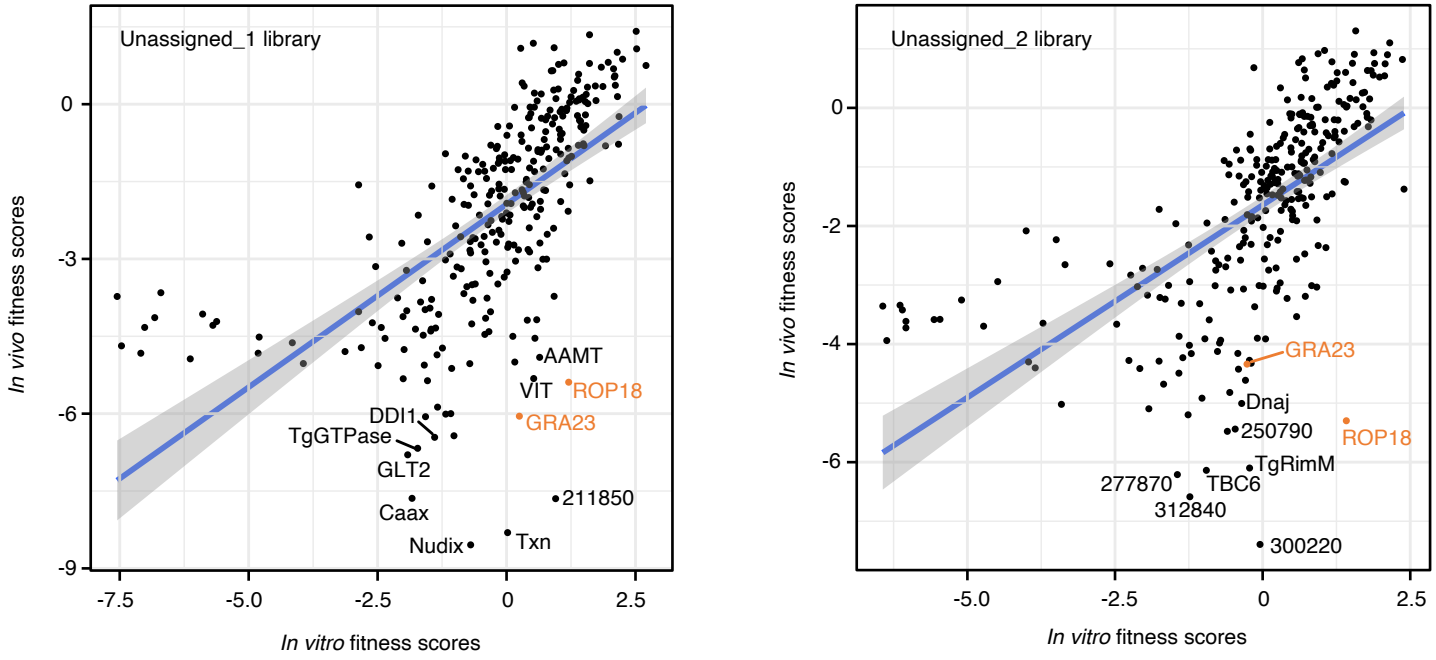

B

Unassigned_1 library

Rank	ID	Gene name	In vitro	In vivo	Distance from line
1	TGGT1_211850	Hypothetical	0.95	-7.65	5.24
2	TGGT1_224060	Txn	0.02	-8.31	5.24
3	TGGT1_282190	Nudix	-0.7	-8.54	5.01
4	TGGT1_221170	Caax	-1.83	-7.64	3.62
5	TGGT1_205250	ROP18	1.2	-5.39	3.54
6	TGGT1_297880	GRA23	0.25	-6.05	3.53
7	TGGT1_237460	Hypothetical	-1.02	-6.43	3.10
8	TGGT1_266800	VIT	0.53	-5.32	3.09
9	TGGT1_304680	DDI1	-1.39	-6.46	2.91
10	TGGT1_277840	TgGTPase	-1.72	-6.67	2.89
11	TGGT1_239752	GLT2	-1.92	-6.8	2.88
12	TGGT1_310070	AAMT	0.64	-4.91	2.82
13	TGGT1_217340	Hypothetical	-1.08	-6.00	2.72
14	TGGT1_221190	mRNACF	-1.18	-6.01	2.67
15	TGGT1_253560	Hypothetical	0.16	-5.00	2.62

Unassigned_2 library

Rank	ID	Gene name	In vitro	In vivo	Distance from line
1	TGGT1_300220	Hypothetical	-0.04	-7.39	4.83
2	TGGT1_205250	ROP18	1.42	-5.30	3.87
3	TGGT1_321310	TgRimM	-0.22	-6.10	3.65
4	TGGT1_312840	Hypothetical	-1.23	-6.59	3.51
5	TGGT1_237280	TBC6	-0.95	-6.14	3.29
6	TGGT1_277870	Hypothetical	-1.44	-6.21	3.08
7	TGGT1_250790	Hypothetical	-0.46	-5.44	2.97
8	TGGT1_221640	Hypothetical	-0.60	-5.48	2.93
9	TGGT1_203380	Dnaj	-0.36	-5.01	2.66
10	TGGT1_267710	CPSF	-0.56	-4.82	2.40
11	TGGT1_249260	CDK	-0.29	-4.61	2.37
12	TGGT1_224600	GTPBP	-1.26	-5.20	2.33
13	TGGT1_240660	EFG1	-1.03	-4.92	2.22
14	TGGT1_273905	Hypothetical	-0.19	-4.32	2.18
15	TGGT1_297880	GRA23	-0.26	-4.34	2.15

Figure 1. *In vivo* CRISPR screening targeting proteins with hyperLOPIT-unassigned localization.

(A) Scatterplots showing *in vitro* and *in vivo* fitness scores from Unnassigned_1 (left) and Unassigned_2 (right) libraries, respectively. ROP18 and GRA23 are labeled in orange as control genes. (B) Ranking tables for top 15 *in vivo* fitness-conferring genes in each library ordered by the distance from the regression line.

Figure 2 _Tachibana et al.

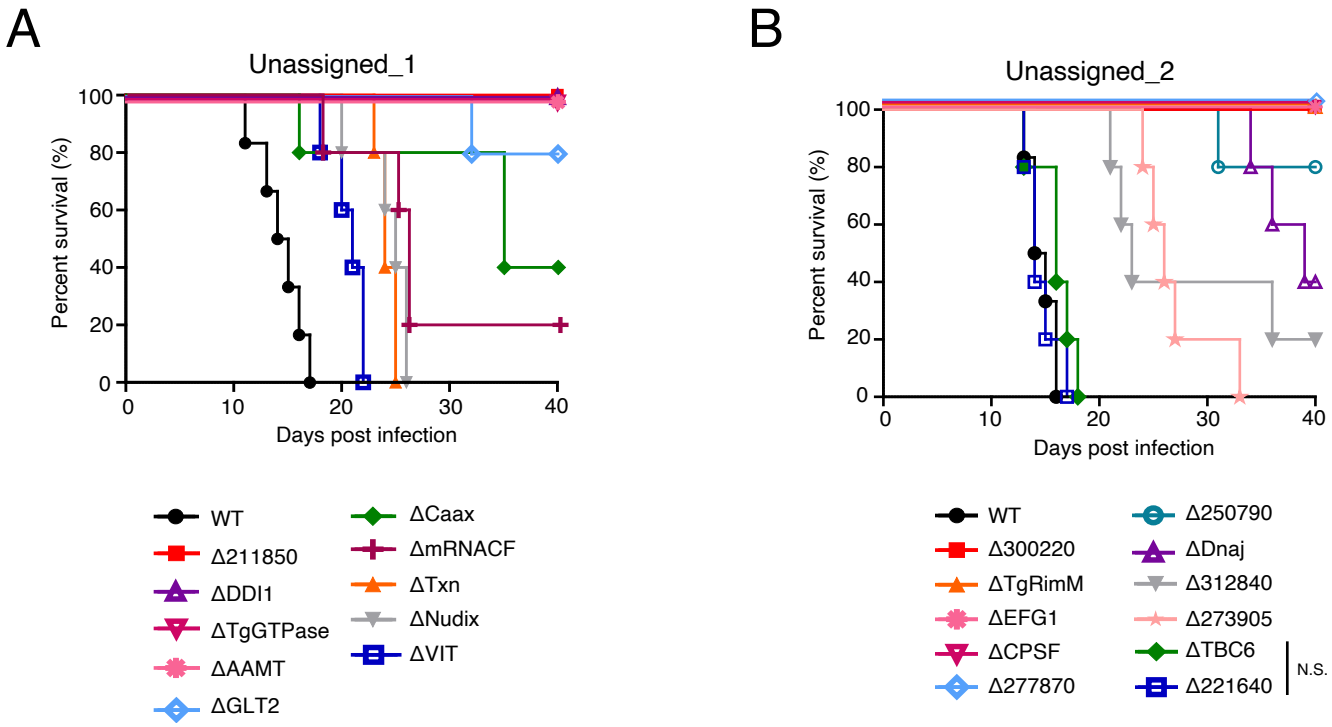

Figure 2. Validation of candidate genes that affect parasite virulence.

(A) C57BL/6 mice were inoculated into the footpad with 10^3 tachyzoites of the indicated knockout strains from the unassigned_1 library. WT (n = 6), ΔTGGT1_211850 (n = 5), ΔDDI1 (n = 5), ΔTgGTPase (n = 5), ΔAAMT (n = 5), ΔGLT2 (n = 5), ΔCaax (n = 5), ΔmRNACF (n = 5), ΔTxn (n = 5), ΔNudix (n = 5), ΔVIT (n = 5).

(B) C57BL/6 mice were inoculated into the footpad with 10^3 tachyzoites of the indicated knockout strains from the unassigned_2 library. WT (n = 6), ΔTGGT1_300220 (n = 5), ΔTgRimM (n = 5), ΔEFG1 (n = 5), ΔCPSF (n = 5), ΔTGGT1_277870 (n = 5), ΔTGGT1_250790 (n = 5), ΔDnaj (n = 5), ΔTGGT1_312840 (n = 5), ΔTGGT1_273905 (n = 5), ΔTBC6 (n = 5), ΔTGGT1_221640 (n = 5). N.S., not significant (log-rank test).

Figure 3 Tachibana et al.

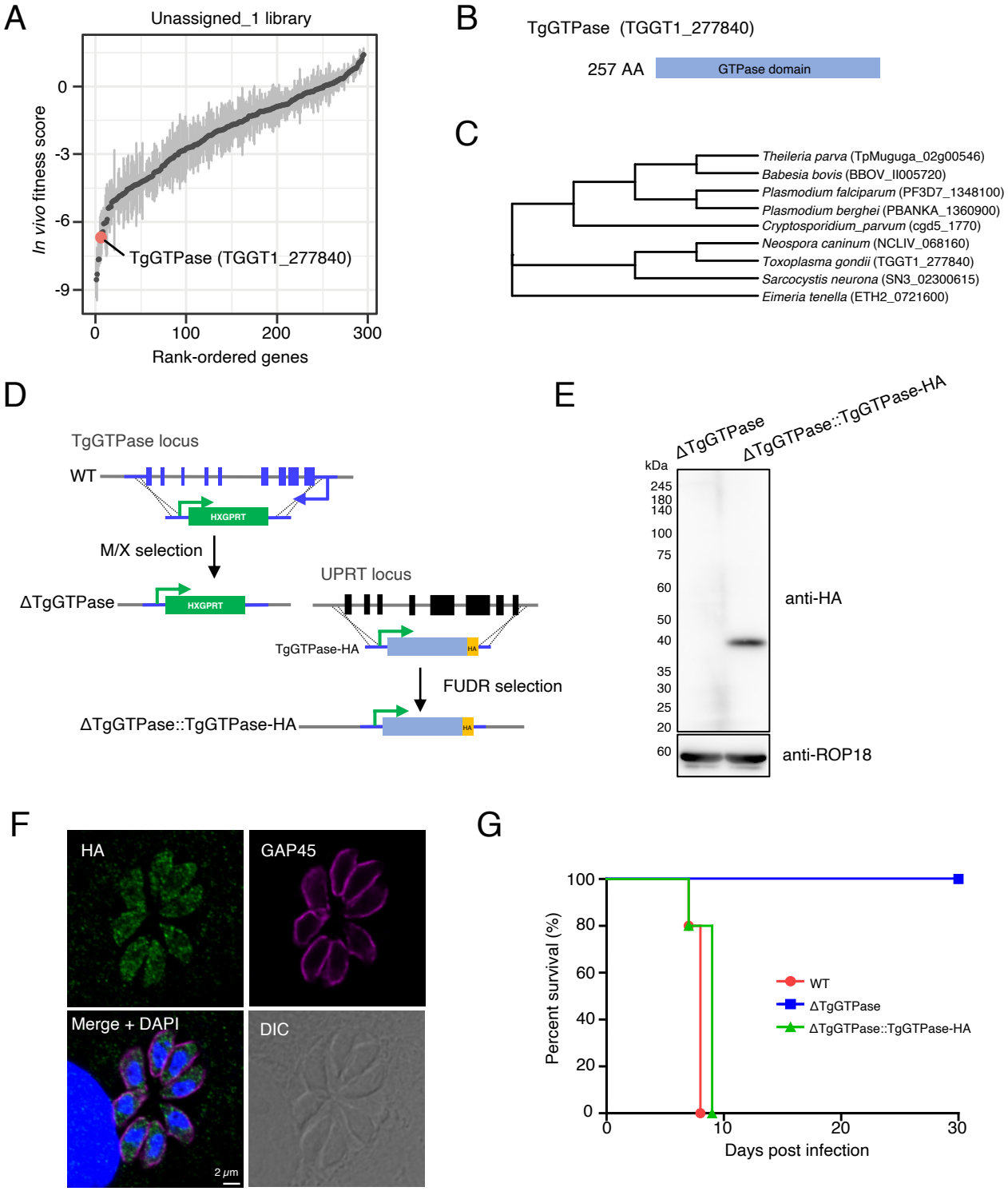

Figure 3. TgGTPase is a cytosolic GTPase that contributes to parasite virulence.

(A) Rank-ordered plot of genes from Unassigned_1 library. (B) Schematic of putative domains in TgGTPase. (C) Phylogenetic tree of selected TgGTPase homologs across the apicomplexan phylum. (D) Schematic of TgGTPase knockout and complementation of TgGTPase-HA. (E) Western blot analysis of TgGTPase-HA. (F) Immunofluorescence images of ΔTgGTPase::TgGTPase-HA showing cytosolic localization of TgGTPase-HA (green). GAP45 (magenta) stains the inner membrane complex of the parasites. (G) Survival curves of C57BL/6 mice intraperitoneally infected with 10^3 tachyzoites of WT (n = 5), ΔTgGTPase (n = 5), and ΔTgGTPase::TgGTPase-HA (n = 5). Data are representative of three independent experiments (E and F).

Figure 4 Tachibana et al.

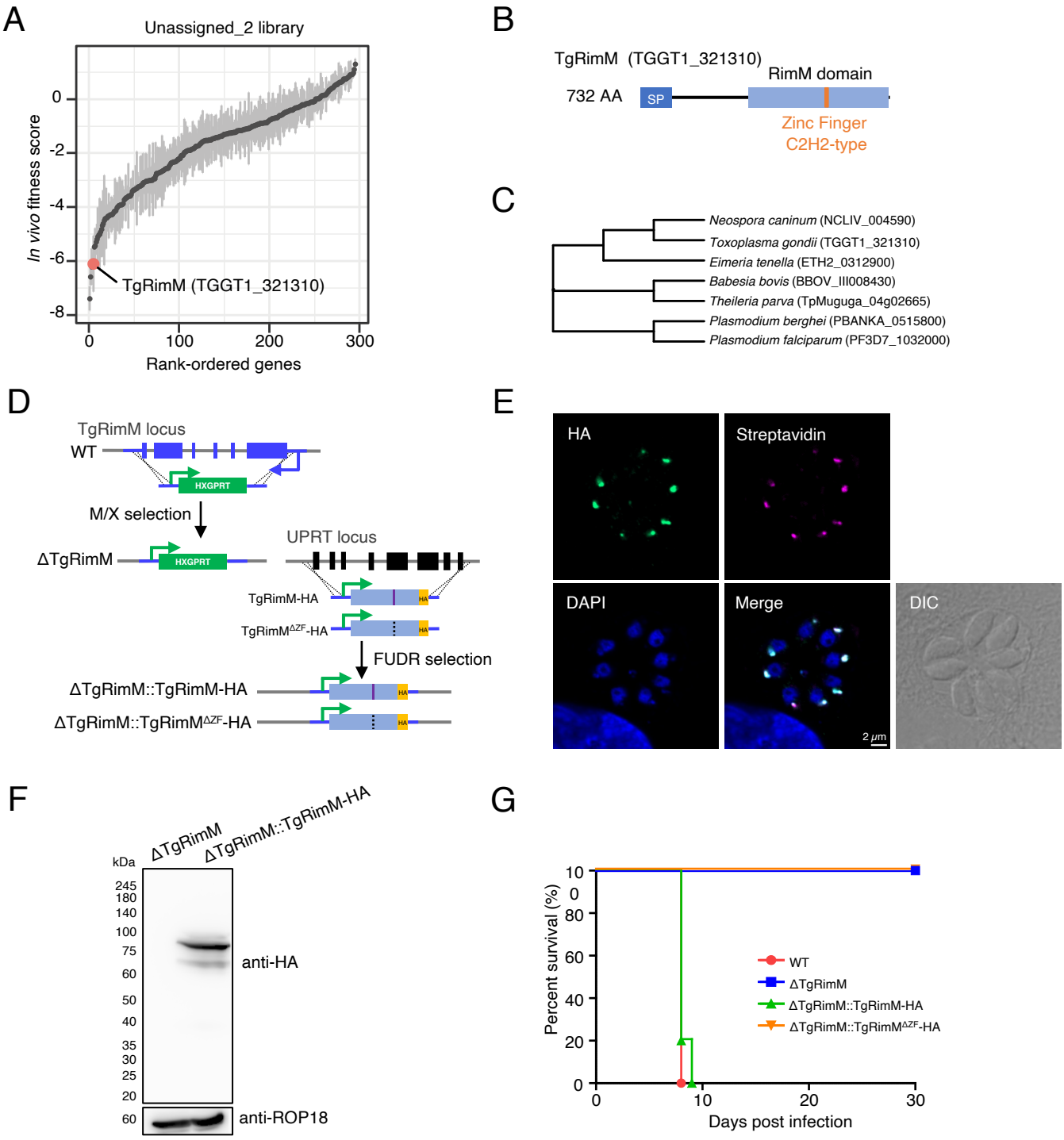

Figure 4. TgRimM is an apicoplast-resident protein that is essential for parasite virulence.

(A) Rank-ordered plot of genes from Unassigned_2 library. (B) Schematic of putative domains in TgRimM. SP is predicted by SignalP 6.0. (C) Phylogenetic tree of selected TgRimM homologs across the apicomplexan phylum. (D) Schematic of TgRimM knockout and complementation of wild-type and mutant TgRimM. (E) Immunofluorescence images of ΔTgRimM::TgRimM-HA showing TgRimM-HA (green) is co-stained with streptavidin (magenta), an apicoplast marker. (F) Western blot analysis of TgRimM-HA. (G) Survival curves of C57BL/6 mice intraperitoneally infected with 10^3 tachyzoites of WT (n = 5), ΔTgRimM (n = 5), ΔTgRimM::TgRimM-HA (n = 5), or ΔTgRimM::TgRimM$^{\Delta ZF}$-HA (n = 5). Data are representative of three independent experiments (E and F).